This is a repository copy of *Spin-orbit torque-driven magnetization switching and thermal effects studied in Ta\CoFeB\MgO nanowires*.

Spin-orbit torque-driven magnetization switching and thermal effects studied in Ta\CoFeB\MgO nanowires

R. Lo Conte[1,3], A. Hrabec[2], A. P. Mihai[2†], T. Schulz[1], S.-J. Noh[1], C. H. Marrows[2], T. A. Moore[2], and M. Kläui[1,3]

[1]*Johannes Gutenberg Universität-Mainz, Institut für Physik, Staudinger Weg 7, 55128 Mainz, Deutschland*
[2]*School of Physics and Astronomy, E. C. Stoner Laboratory, University of Leeds, Leeds LS2 9JT, U.K.*
[3]*Graduate School of Excellence Materials Science in Mainz (MAINZ), Staudinger Weg 9, 55128 Mainz, Deutschland*
[†]*now at: Imperial College, South Kensington Campus, London SW7 2AZ, UK*

We demonstrate magnetization switching in out-of-plane magnetized Ta\CoFeB\MgO nanowires by current pulse injection along the nanowires, both with and without a constant and uniform magnetic field collinear to the current direction. We deduce that an effective torque arising from spin-orbit effects in the multilayer drives the switching mechanism. While the generation of a component of the magnetization along the current direction is crucial for the switching to occur, we observe that even without a longitudinal field thermally generated magnetization fluctuations can lead to switching. Analysis using a generalized Néel-Brown model enables key parameters of the thermally induced spin-orbit torques-driven switching process to be estimated, such as the attempt frequency and the effective energy barrier.

Nowadays a large effort is focused on the investigation of promising magnetic materials systems in order to find good candidates for future logic circuits and memory devices. A continuous and growing interest in *spin-orbit torque* (SOT)-driven magnetization dynamics results from the possibility of using this torque in prospective spintronic devices based on ultra-fast current-induced domain wall motion[1] or fast current-induced magnetization switching[2]. The origin of these torques in perpendicularly magnetized multilayers with structural inversion asymmetry (SIA) such as Pt\Co\AlOx[3-7] or Ta\CoFe\MgO[8] seems to be spin-orbit effects generated when an electric current is injected through them. One of the two proposed underlying mechanisms is the Rashba effect[4-6,9,10], which generates an in-plane effective magnetic field perpendicular to both the current-flow and the out-of-plane axis. The second proposed mechanism is the spin Hall effect (SHE)[8,11-14], which generates a pure spin-current that diffuses across the heavy metal-ferromagnet interface. Such a spin-current has an in-plane spin polarization, which is able to exert a torque on the magnetic texture present in the ferromagnetic layer. However, the debate about the detailed origin of the torques in the different materials stacks is still open. Systems made of Ta\CoFeB\MgO are of particular interest as such a trilayer is already used as a bottom electrode in existing spintronic devices based on CoFeB\MgO\CoFeB magnetic tunnel junctions (MTJs)[15]. The main issue with such devices is the possible damage of the MTJ due to the injection of current across the tunnel barrier, in order to obtain spin-transfer torque (STT)-driven magnetization switching[16]. However, this risk could be mitigated using a three terminal device where switching is driven by SOTs produced by current flowing in plane[17]. In this case only a small read-out current would flow through the tunnel junction - reducing the risk of structural damage to the insulating barrier from high voltages and currents, and making it possible to scale down the cross-section of the MTJs.

Even if the switching of structures using SOTs has been investigated previously[6,7,8,11], it was only achieved when an additional longitudinal magnetic field was applied, which is cumbersome for real applications. Additionally, the current is expected to generate Joule heating, so thermal effects, which have not yet been investigated in detail, can be expected to play a role in the SOT-driven magnetization switching.

In this letter, we demonstrate magnetization switching of out-of-plane magnetized Ta\CoFeB\MgO nanowires by current pulse injection along the nanowires. Switching is obtained both with and without a constant and uniform external in-plane magnetic field collinear to the current direction. Current pulses of different time-length and of different polarity are used to obtain switching of the magnetization of the nanowires. The effects of thermal fluctuations in the switching process are analyzed based on a generalized Néel-Brown model and this allows key parameters, such as the attempt frequency and the energy barrier for the switching process, to be determined.

Our samples consist of a Ta(5nm)\Co$_{20}$Fe$_{60}$B$_{20}$(1nm)\MgO(2nm)\Ta(5nm)-multilayer deposited on a thermally oxidized Si-wafer. All the layers are deposited by sputtering technique (using a Singulus TIMARIS/ROTARIS tool), followed by annealing at 300 ^{o}C for 2 hours in order to obtain a large perpendicular magnetic anisotropy. The samples are then patterned into an array of 20 nanowires in a parallel configuration (see Fig. 1) by electron-beam lithography and argon-ion milling. Each nanowire is 1 µm wide and 8 µm long. At both ends of the nanowires there are two magnetic pads, directly connected to two gold pads made in a second optical lithography step. The electrical resistivity of the devices is around 160 nΩm. As illustrated in Fig. 1, during the measurements the device is electrically connected in series to a pulse generator on one side, and to an oscilloscope on the other. A voltage pulse is applied to the sample and the pulse waveform is measured by the oscilloscope across its 50 Ω-internal resistance (R_0). The current flowing through the system is obtained by the measured voltage (V_o) across R_0. Considering that of the Ta-capping layer only about 3 nm are still conducting due to surface oxidation, we estimate the current density as follows: for 1 V dropping across R_0 (corresponding to a total current of 20 mA) we have a current density of 1.1×10^{11} A/m^2 flowing through the nanowires of our system. The magnetization state of the nanowires is imaged by differential polar Kerr microscopy. The microscope is also equipped with an in-plane coil for the generation of an external in-plane magnetic field. During our experiment carried out at T=300 K, we first saturate the magnetic nanowires in the up (+z)- or down (-z)-magnetization state in an external field, then we apply a constant and uniform in-plane magnetic field µ$_0$**H$_x$** along the nanowires. After the injection of a current pulse through the device, the magnetization of the nanowires is switched for appropriately chosen field and current density[7,8]. Each magnetization switching event is observed directly using a Kerr microscope, after the current pulse injection (Figs. 1(b), and 1(c)).

In Fig. 2 we show the magnetization switching for 100 ns (closed symbols)- and 100 ms (open symbols)-long current pulses, when a constant and uniform external magnetic field µ$_0$**H$_x$** is applied along the nanowire direction. For both the 100 ns- and 100 ms-long pulses we determine the minimum current amplitude needed to obtain magnetization switching in combination with a fixed external magnetic field value (see Fig. 2(a)). The magnetization switching condition is defined as switching in at least half of the total number of pre-saturated

nanowires. In Fig. 2(a) we can see that there is a clear link between the current needed for the switching to occur and the applied in plane field. The lower the in-plane field, the larger is the necessary amplitude of the current pulse. This is qualitatively in agreement with the model of the spin-orbit effective field reported by Emori et al.[8], where $\boldsymbol{H_{SHE}} = \hbar\theta_{SHE}|j_e|/(2\mu_0|e|M_s t_f)(\hat{\boldsymbol{m}} \times (\hat{\boldsymbol{z}} \times \hat{\boldsymbol{j_e}}))$, and θ_{SHE} is the spin Hall angle, j_e the electron-current density, M_s the saturation magnetization of the ferromagnetic material and t_f the thickness of the ferromagnetic layer. The effective spin-orbit field is also a function of the sign of the current, so that it can work with the external field (leading to a switching event) or against it (keeping the magnetization state in the initial one).

Next, we compare the results obtained for the two different pulse lengths. First of all we find that the amplitude of the short current pulses required for switching is about 3 times larger than is the case for long pulses, for a fixed value of H_x. Furthermore, we find also that for the long pulses we observe a saturation of the current needed for switching for values of $\mu_0 H_x$ lower than 50 mT (see guide lines in Fig. 2 (a)). These observations clearly point to thermal effects playing a crucial role. Our interpretation is that for large enough current amplitudes, the thermal fluctuations of **M** start to generate an in-plane component of **M**, which becomes comparable to that generated by an external field. When a large enough M_x component is eventually thermally generated in the correct direction, a spin-orbit effective field acts on it yielding a magnetization switching in part of the nanowire and then a complete switching by fast domain wall motion[7]. During the injection of long pulses there is much more time for the thermally induced switching to occur than in the case of the short pulses, increasing the switching probability and thus reducing the necessary in-plane current. This explains why, even at large pulse amplitudes, we do not observe this saturation effect for short pulses. It follows that, for sufficiently high current density, we might expect thermal fluctuations to become large enough to trigger the switch of the magnetization even without any applied in-plane field, and we investigate this in the last part of this letter. Fig. 2(b) shows the stable magnetization configurations as a function of current sign and field orientation. We can see that for both I_p and H_x positive or negative the stable magnetization configuration is M+ (up), while for I_p and H_x of opposite sign the stable magnetization state is M- (down). This result confirms the fact that the switching effect is strictly linked to the spin-current generated in the heavy metal when an electric current is injected in plane through the stack[7,8,17,18]. This is also in agreement with the observation in systems made of Ta\CoFe\MgO[8], confirming that the sign of θ_{SHE} in Ta is negative[17].

To test our interpretation of thermally activated switching, we measure the length Δt_{pulse} of the current pulse needed to switch the magnetization in our system, using a fixed current density of 7×10^{11} A/m^2 (see Fig. 3). These measurements are done on a second sample, made of the very same materials stack and with the same dimensions reported above. The experiment is carried out with different values of the external magnetic field, measuring the minimum Δt_{pulse} needed for a 10%, 30% and 50% (effectively 49% for the zero field case, due to the fact that 50% is the asymptotic limit in that case) probability of switching. The switching probability is proportional to the total switched area in the observed NWs. This means that if all the NWs are completely switched, a 100% switching event is observed. Fig. 3 shows that there is an exponential dependence of the Δt_{pulse} on the external magnetic field $\mu_0 H_x$, for all the three different switching probabilities here reported. The lower the applied in-plane field, the longer is the current pulse needed for switching. For $\mu_0 H_x$=0 mT we observe a 10%, 30% or >49% magnetization switching starting from a pulse length of 17 ns, 18 ns or 23 ns respectively. To obtain the key parameters for the thermally activated switching, we fit our experimental data with a generalized Néel-Brown model[19]. This model describes the role of the thermal fluctuations in magnetization switching processes, in the presence of a spin-transfer torque. In our experiment we have a similar situation, with an electric current flowing in the system and a spin-current pumped in the magnetic layer due to the SHE, resulting in a non-equilibrium condition. The equation that describes our experiment is the following[19]:

$$\Delta t_{pulse} = -\ln(1-P)f_0^{-1}\exp\left(\frac{E_0^*}{k_B T}\left(1 - \frac{H_z}{H_{sw}^0}\right)^{1.5}\right)$$

where P is the switching probability, f_o is the attempt frequency, $E_o^*=E_o(1-\alpha I)$ (I is the current flowing in the system, α is a coefficient) is the effective energy barrier at the given current, $\mu_o H^\circ_{sw}$ is the switching field at 0 K, and $\mu_o H_z$ is the effective field along the easy axis. In our case the field along the z-direction is the spin-orbit field $H_z = \frac{\hbar\theta_{SHE}|j_e|}{2\mu_0|e|M_s t_f}m_x = \frac{\hbar\theta_{SHE}|j_e|}{2\mu_0|e|M_s t_f}\frac{H_x}{H_x^{sat}}$, where $\mu_o H_x^{sat}$ is the longitudinal field needed for aligning all the magnetization in the x-direction ($\approx$ 400 mT in our system). As can be seen in Fig. 3, the model (solid lines) fits the data well for a value of the effective energy barrier $E_o^* \approx$ 90 meV. The extracted average attempt frequency is: $f_o \approx$ 1.4 GHz. We also carried out the same experiment with the sample used for the measurements reported in Fig. 2 for 50% switching probability, and we observe a similar value for the effective energy barrier

(~88 meV). The value reported above for E_o^* is a lower boundary of the actual energy barrier E_0, due to the fact that the electric current and the spin-current flowing in the magnetic layer reduce its effective value, due mainly to the increase in temperature generated in the system. From measurements of the sample resistance as a function of the temperature and of the current density during current injection[20], we deduce that the actual temperature in the nanowires during the pulse injection for the experiment described above is well below the expected Curie temperature of our magnetic material[21], that is ~1030 K (for annealed $Co_{20}Fe_{60}B_{20}$) as reported by M. Yamanouchi et al.[22].

The fitting curves have an off-set of 10 ns which is the sum of two potential contributions. One contribution is from the shape of the pulses we are able to apply with our set-up. For this specific experiment, we have a rise- and a fall-time of about 2 ns each. This means that the current density is actually at its maximum value for at least 4 ns less than the nominal duration of the pulse. Secondly, we assume a 100% switching in each NW when the magnetization is reversed throughout its length. For a switching mechanism based on domain nucleation followed by domain wall motion[7], part of the minimum time obtained from the fitting curve could also be due to the fact that the domain walls need some time to move to the end of the nanowires. The calculated domain wall speed is in the order of hundreds of m/s, which is in line with the velocities measured for similar materials stacks[3-5].

Finally, we note that this thermally activated switching is not unidirectional, since in the absence of the magnetic field the spin-orbit torque would destabilize the magnetization configuration every time a current pulse is injected in the system. This means we can obtain switching in both directions using the same current pulse polarity. For applications it implies that one would need to read after writing to check that the writing process actually occurred.

In summary, we have demonstrated SOT-driven magnetization switching in nanowires made of Ta\CoFeB\MgO. The switching was observed to depend on the pulse length for 100 ns- and 100 ms-long current pulses in the current density range of 10^{11} A/m^2 due to thermal effects. Pure current-induced magnetization switching in absence of external magnetic field applied was obtained for 23 ns-long pulses at 7×10^{11} A/m^2, with a 50% probability. Our experimental data are reproduced by employing the generalized Néel-Brown model, enabling the attempt frequency and the effective energy barrier to be extracted. While this approach allows us to switch magnetization even without any field, it requires a subsequent read-out to confirm switching for the use in devices.

Fig. 1 (a) Schematic of the experimental set-up for current pulse injection, including an SEM micrograph of the Ta\CoFeB\MgO nanowires. The inset shows the shape of one of the voltage pulses applied to the device, measured with the oscilloscope (across the 50 Ω internal resistance). **(b)** Differential Kerr microscopy image of the initialized nanowires with the magnetization pointing down (-z) everywhere. **(c)** Differential Kerr microscopy image of the same nanowires in (b), after their magnetization has been switched up (+z) by a current pulse in the presence of an in-plane magnetic field collinear with the current-flow.
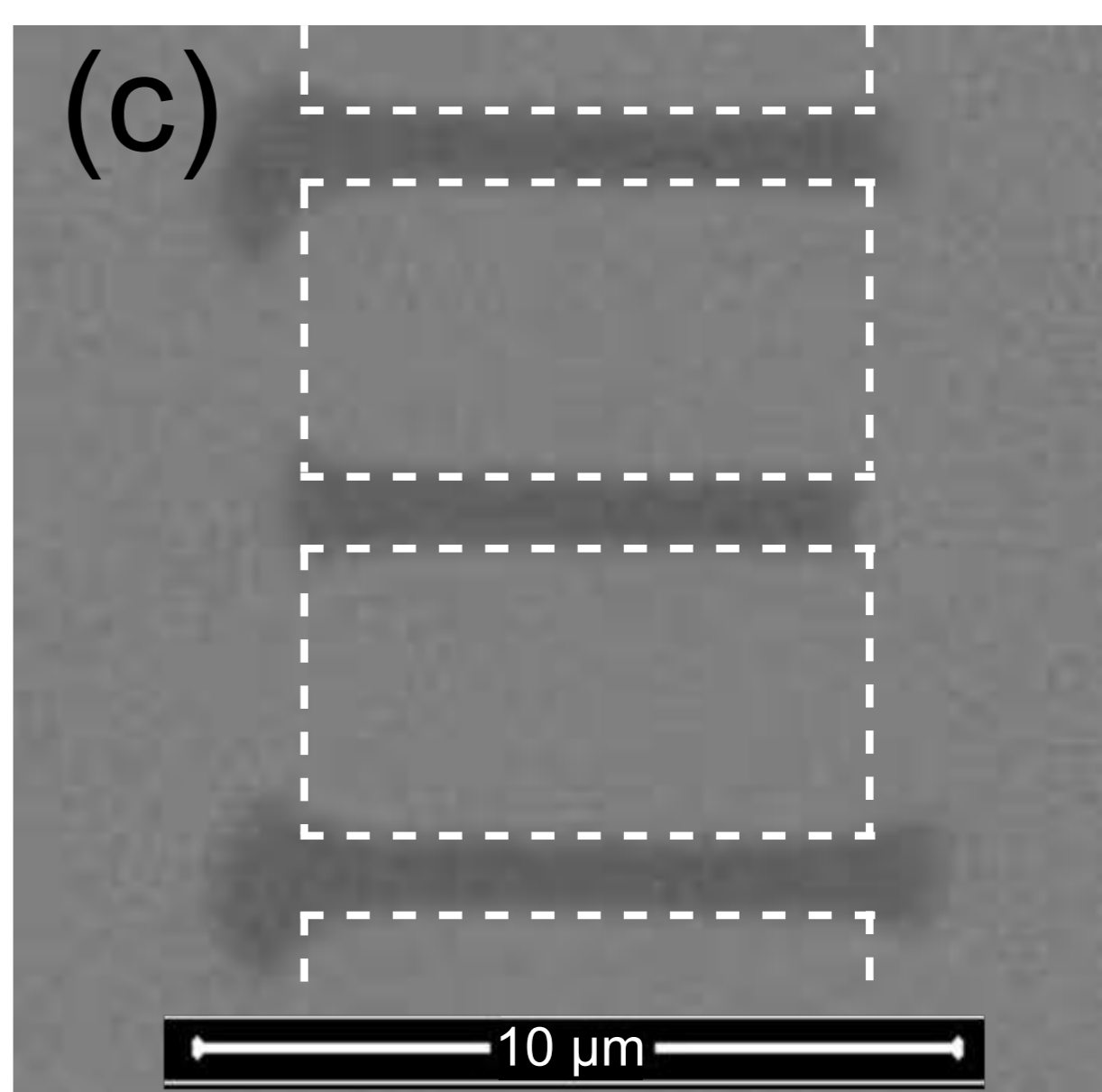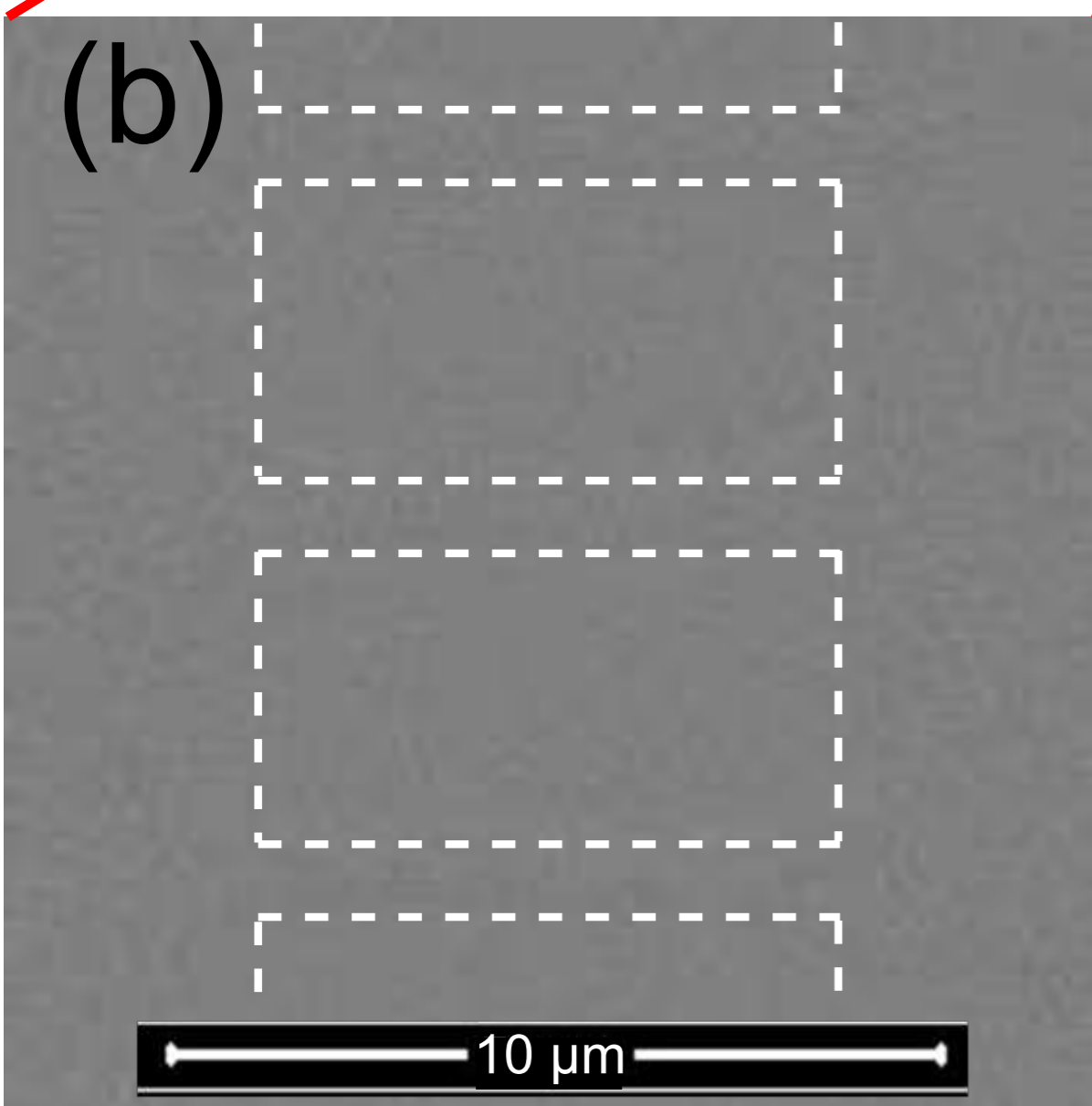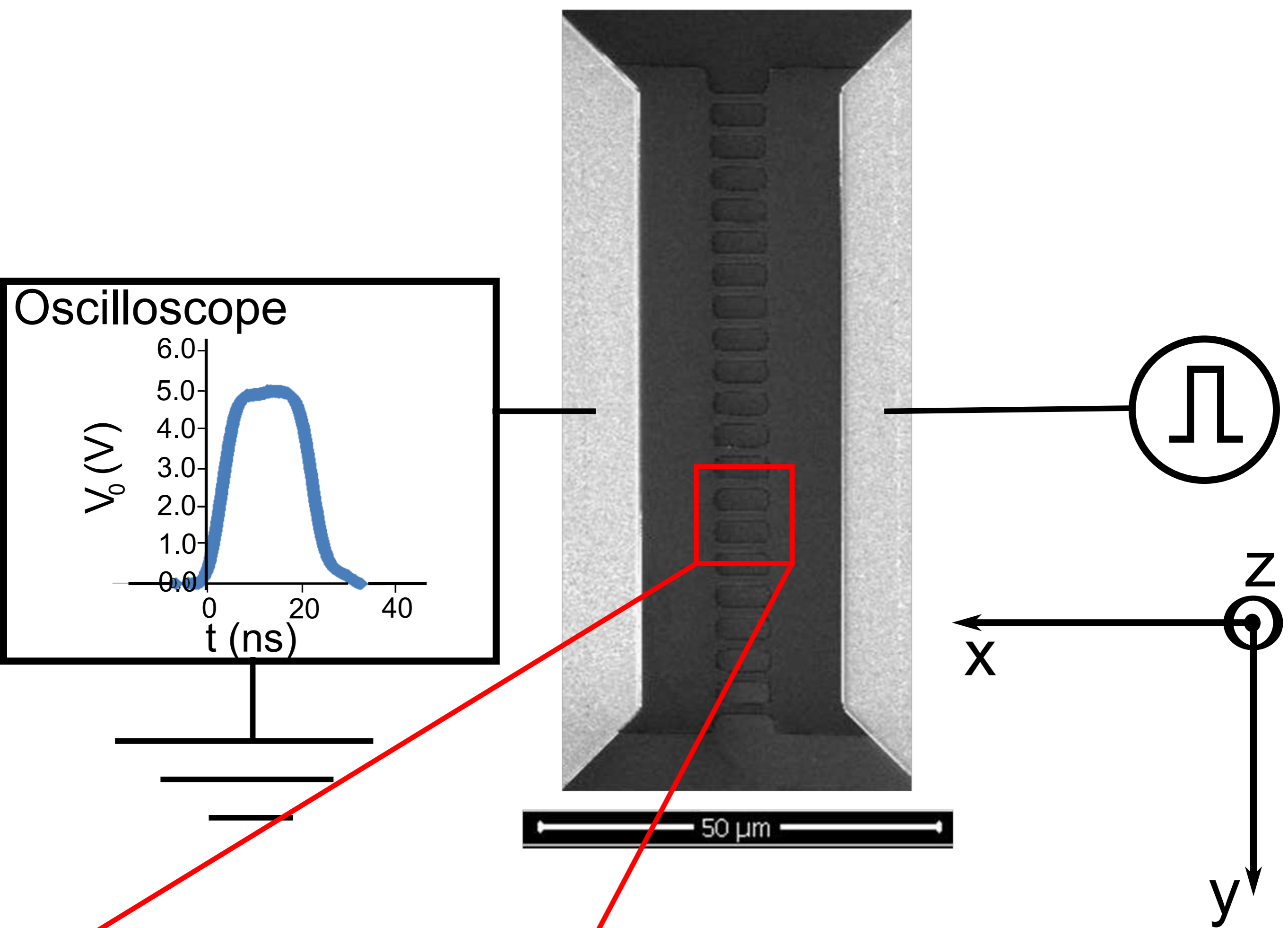
Fig. 2 (a) Minimum current density (**J**) needed to switch the magnetization in at least half of the nanowires (10 of 20) for a fixed longitudinal in-plane magnetic field ($\mathbf{\mu_0 H_x}$). The closed (open) symbols show the switching events due to 100 ns- (100 ms-) long current pulses. The squares (triangles) show the Down → Up (Up → Down) switching events. The lines are a guide to the eye, highlighting the saturation of the required switching current density at low magnetic fields in the case of long pulses. **(b)** Stable magnetization states for the four different field-current combinations: M+ (+z-direction), M- (-z-direction).
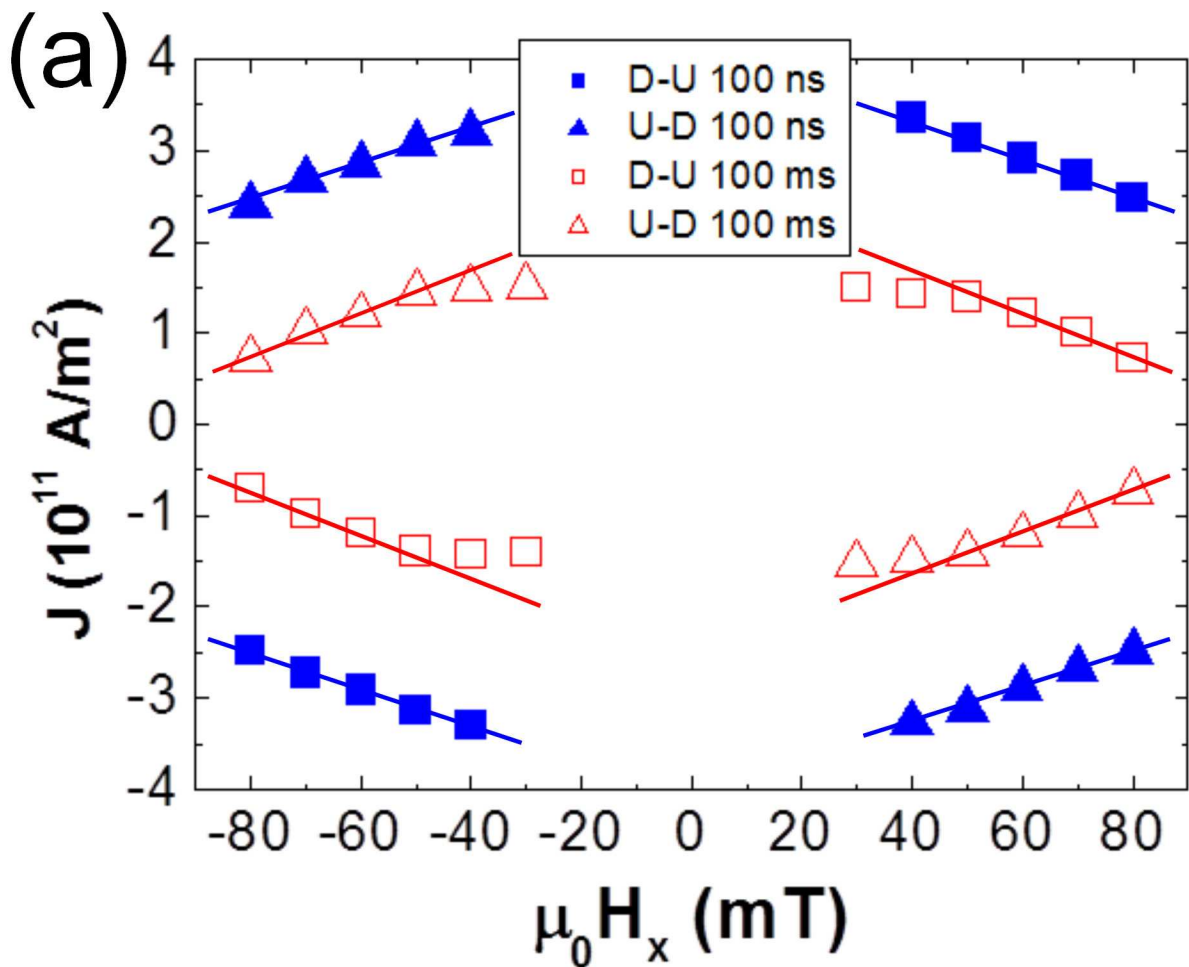
Fig. 3 Minimum length of the current pulse needed in order to switch the magnetization in the nanowires of the sample with a probability of 10% (blue dots), 30% (green diamonds) and 50% (red stars), as function of the longitudinal magnetic field. The pulse current density is 7×10^{11} A/m^2. The error bar corresponds to 0.25 ns, which is the difference between two consecutive pulse lengths used during the measurements. The fitting curves are based on the generalized Néel-Brown model for thermally-assisted magnetization switching.

References

[1] S. S. P. Parkin, M. Hayashi, and L. Thomas, Science **320**, 190 (2008).

[2] S.Ikeda, J.Hayakawa, Y. M. Lee, F. Matsukura, Y. Ohno, T. Hanyu, and H. Ohno, IEEE Trans. Electron Devices **54**(5) 991-1002 (2007).

[3] T. A. Moore, I. M. Miron, G. Gaudin, G. Serret, S. Auffret, B. Rodmacq, A. Schuhl, S. Pizzini, J. Vogel, and M. Bonfim, Appl. Phys. Lett. **93**, 262504 (2008).

[4] I. M. Miron, G. Gaudin, S. Auffret, B. Rodmacq, A. Schuhl, S. Pizzini, J. Vogel, and P. Gambardella, Nature Mat. **9**, 230-234 (2010).

[5] I. M. Miron, T. Moore, H. Szambolics, L. D. Buda-Prejbeanu, S. Auffret, B. Rodmacq, S. Pizzini, J. Vogel, M. Bonfim, A. Schuhl and G. Gaudin, Nature Mat. **10**, 419-423 (2011).

[6] I. M. Miron, K. Garello, G. Gaudin, P. J. Zermatten, M. V. Costache, S. Auffret, S. Bandiera, B. Rodmacq, A. Schuhl and P. Gambardella, Nature **476**, 189-194 (2011).

[7] K. Garello, C. O. Avci, I. M. Miron, O. Boulle, S. Auffret, P. Gambardella, and G. Gaudin, arXiv:1310.5586 **[cond-mat.mes-hall]** (2013).

[8] S. Emori, U. Bauer, S.-M. Ahn, E. Martinez, and G. S. D. Beach, Nature Mat. **12**, 611-616 (2013).

[9] Y. A. Bychkov, and E. I. Rashba, J. Phys. C.: Solid State Phys. **17**, 6039-6045 (1984).

[10] D. A. Pesin, and A. H. MacDonald, Phys. Rew. B **86**, 014416 (2012).

[11] L. Liu, O. J. Lee, T. J. Gudmundsen, D. C. Ralph, and R. A. Buhrman, Phys. Rev. Lett. **109**, 096602 (2012).

[12] M. I. D'yakonov, and V. I. Perel, ZhETF Pis. Red. 13., No. 11, 657-660 (1971).

[13] M. I. D'yakonov, and V. I. Perel, Phys. Lett. **35A**, n. 6 (1971).

[14] A. Manchon, arXiv:1204.4869 **[cond-mat.mes-hall]** (2012).

[15] W. S. Zhao, T. Devolder, Y. Lakys, J. O. Klein, C. Chappert, and P. Mazoyer, Microelectronics Reliability **51**, 1454-1458 (2011).

[16] J. A. Katine and E. E. Fullerton, J. Magn. Magn. Mater. **320** (7), 1217-1226 (2008).

[17] L. Liu, C.-F. Pai, Y. Li, H. W. Tseng, D. C. Ralph, and R. A. Buhrman, Science **336**, 555 (2012).

[18] C. O. Avci, K. Garello, I. M. Miron, G. Gaudin, S. Auffret, O. Boulle, and P. Gambardella, Appl. Phys. Lett. **100**, 212404 (2012).

[19] Z. Li and S. Zhang, Phys. Rev. B **69**, 134416 (2004).

[20] M. Laufenberg, W. Bührer, D. Bedau, P.-E. Melchy, M. Kläui, L. Vila, G. Faini, C.A.F. Vaz, J.A.C. Bland and U. Rüdiger, Phys. Rev. Lett. **97**, 046602 (2006).

[21] See supplementary material at [URL] for the temperature estimation in the nanowires during pulse injection.

[22] M. Yamanouchi, A. Jander, P. Dhagat, S. Ikeda, F. Matsukura, and H. Ohno, IEEE Magn. Lett. **2**, 3000304 (2011).

(a)

Oscilloscope

(b)

(c)

(a)

Legend:
- ■ D-U 100 ns
- ▲ U-D 100 ns
- □ D-U 100 ms
- △ U-D 100 ms

(b)

	$I > 0$	$I < 0$
$H_x > 0$	M+	M−
$H_x < 0$	M−	M+